ASIA PACIFIC JOURNAL OF MARKETING & MANAGEMENT REVIEW
ISSN: 2319-2836
IMPACT FACTOR: 7.603
Vol 12, Issue 11, 2023

AUTONOMOUS SOLAR OPTRON BASED ON AFN PHOTODETECTOR

Kuldashov G.O., Ergashev Sh.U.
Fergana branch of Tashkent University of Information Technologies
e-mail: ergashevshoh1992@gmail.com

Annotation: This paper discusses a detailed description of the design of a special physical device of a helioptocoupler aimed at receiving solar radiation with its subsequent conversion, as well as output in the form of an anomalously high photo-voltage.

All processes are considered from the point of view of physical and mathematical modeling and detailed analysis of the physical processes used in the design.

The analysis from the calculation and design side coincides with the general description of the design of the solar optron device.

Key words: solar optron, detailed analysis, APS films, anomalous photovoltage, physical and mathematical modeling, generation, solar radiation.

Introduction

The entire device of a solar optocoupler includes a whole circuit, presented in the form (Fig. 1), where there are a large number of very different components, which are worth discussing in detail, just like all the physical methods that are actively used during their operation [1-3].

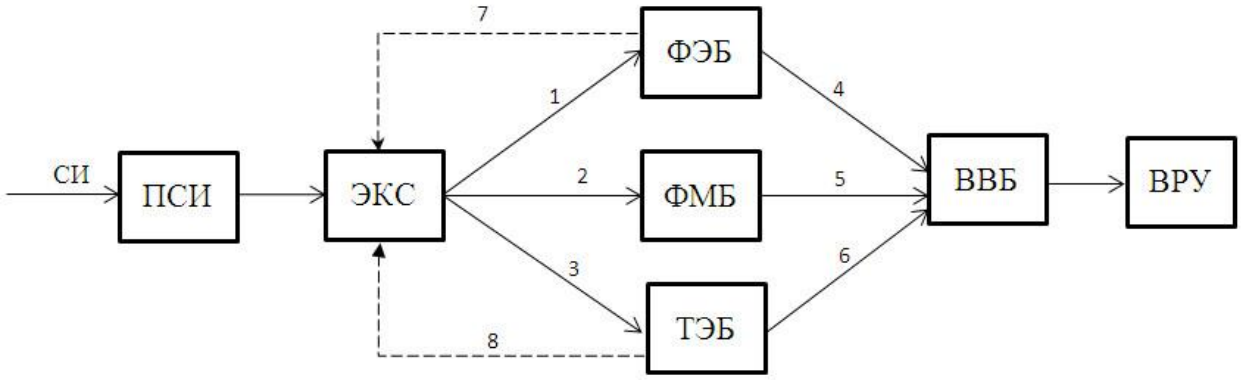

Rice. 1. Diagram of the solar optocoupler device, 1, 2, 3 – optoelectronic circuits, 4, 5, 6 – electrical connecting circuits, 7, 8 – electrical circuits for feedback, VVB – high-voltage unit, FEB – photovoltaic unit,
TEB – thermoelectric block, FMB – photo-magnetic-electric block,
PSI – solar radiation receiver, EX – electronic switching system, ASU – output operating device with dielectric load, SI – solar radiation, OBS – feedback.

Guided radiation

The design of the device initially begins with the direction of solar radiation to a special receiver, which is a technology for increasing the luminous flux, after which it is directed towards the electronic switching system of the solar optron. Let's consider the physical and mathematical modeling of the process of increasing the light directed flux of solar radiation. It is worth noting the

ISSN 2319-2836 (online), Published by
ASIA PACIFIC JOURNAL OF MARKETING & MANAGEMENT REVIEW.,
under Volume: 12 Issue: 11 in November-2023
https://www.gejournal.net/index.php/APJMMR

ASIA PACIFIC JOURNAL OF MARKETING & MANAGEMENT REVIEW
ISSN: 2319-2836
IMPACT FACTOR: 7.603
Vol 12, Issue 11, 2023

fact that by its nature it consists of a connection of almost all wavelengths, carrying a certain energy value, now defined as a constant - 1,367 W/m2, and already after passing through the atmosphere – 1,020 W/m2 at the equator.

However, here it is necessary to take into account that this value is peak at the equator at noon, when at the time of twilight or sunrise this value decreases to 420 W/m2 [4-6]. The same circumstance should be taken into account when indicating the distance of the point where the measurement is to be made from the equator, where the peak values are known, and closer to the poles this value comes down to 400 W/m2 at noon, and in the early morning or late evening it goes up to 170 W/m2.

To prove this statement, we assume that the given empirical data fits into a plane with the canonical equation (1) and the definition of coordinates (2), where the first indicators are the central angle of deviation from the equator, where it is assumed that the zero value along the abscissa is this is an indication of the time at noon, as a setting of the prime meridian at this time, and as an ordinate, an indication of the corresponding longitude or, more precisely, the sine of this value, which also corresponds to the maxima of the indicated points.

$$Ax + By + Cz + D = 0 \quad (1)$$

$$(0;0;1020), (0;1;400), (1;0;420), (1;1;170) \quad (2)$$

From the above definitions, it becomes sufficient to substitute the presented values into the transition equation in the form of a system of equations, which can be, for solution by the Gaussian method [7,8], transformed into a 5 by 4 matrix in (3).

$$\begin{cases} 0A + 0B + 1020C + D = 0 \\ 0A + B + 400C + D = 0 \\ A + 0B + 420C + D = 0 \\ A + B + 170C + D = 0 \end{cases} => \begin{pmatrix} 0 & 0 & 1020 & 1 & 0 \\ 0 & 1 & 400 & 1 & 0 \\ 1 & 0 & 420 & 1 & 0 \\ 1 & 1 & 170 & 1 & 0 \end{pmatrix} \quad (3)$$

To solve this matrix, we initially change rows 1 and 3, and then from 4 we subtract 1 row, reduced by 1, then from row 4 we subtract row 2, also reduced by 1 (4).

$$=> \begin{pmatrix} 0 & 0 & 1020 & 1 & 0 \\ 0 & 1 & 400 & 1 & 0 \\ 1 & 0 & 420 & 1 & 0 \\ 1 & 1 & 170 & 1 & 0 \end{pmatrix} => \begin{pmatrix} 0 & 0 & 1020 & 1 & 0 \\ 0 & 1 & 400 & 1 & 0 \\ 1 & 0 & 420 & 1 & 0 \\ 0 & 1 & -250 & 0 & 0 \end{pmatrix} =>$$

$$=> \begin{pmatrix} 1 & 0 & 420 & 1 & 0 \\ 0 & 1 & 400 & 1 & 0 \\ 0 & 0 & 1020 & 1 & 0 \\ 0 & 0 & -650 & -1 & 0 \end{pmatrix} \quad (4)$$

The next step towards finding a solution is to divide line 3 by 1020, after which from line 1 we subtract line 3 multiplied by 420, and from line 2 we subtract 3 multiplied by 400, and to line 4 we add line 3 multiplied by 650 (5).

ISSN 2319-2836 (online), Published by
ASIA PACIFIC JOURNAL OF MARKETING & MANAGEMENT REVIEW.,
under Volume: 12 Issue: 11 in November-2023
https://www.gejournal.net/index.php/APJMMR

ASIA PACIFIC JOURNAL OF MARKETING & MANAGEMENT REVIEW
ISSN: 2319-2836
IMPACT FACTOR: 7.603
Vol 12, Issue 11, 2023

$$\begin{pmatrix} 1 & 0 & 420 & 1 & 0 \\ 0 & 1 & 400 & 1 & 0 \\ 0 & 0 & 1 & \frac{1}{1020} & 0 \\ 0 & 0 & -650 & -1 & 0 \end{pmatrix} => \begin{pmatrix} 1 & 0 & 0 & \frac{10}{17} & 0 \\ 0 & 1 & 0 & \frac{31}{51} & 0 \\ 0 & 0 & 1 & \frac{1}{1020} & 0 \\ 0 & 0 & 0 & -\frac{37}{102} & 0 \end{pmatrix} \quad (5)$$

Then it becomes necessary that the 4th line is divided by the negative ratio of 37 and 102, after which the 4th line is subtracted from the 1st line, multiplied by the ratio of 10 to 17, and the 4th line is subtracted from the 2nd line, multiplied by the ratio of 31 to 51, then from the 3rd line the 4th line is subtracted, multiplied by the ratio of 1 to 1020 (6).

$$\begin{pmatrix} 1 & 0 & 0 & \frac{10}{17} & 0 \\ 0 & 1 & 0 & \frac{31}{51} & 0 \\ 0 & 0 & 1 & \frac{1}{1020} & 0 \\ 0 & 0 & 0 & 1 & 0 \end{pmatrix} => \begin{pmatrix} 1 & 0 & 0 & 0 & 0 \\ 0 & 1 & 0 & 0 & 0 \\ 0 & 0 & 1 & 0 & 0 \\ 0 & 0 & 0 & 1 & 0 \end{pmatrix} \quad (6)$$

Thus, by simply transforming the resulting matrix back into a system of equations, it was possible to arrive at a trivial solution (7), which has no physical meaning.

$$(0; 0; 0; 0) \quad (7)$$

It is worth noting that the surface was previously assumed to be of first order and it is appropriate to assume that when taking indicators relative to other coordinates (9), taking into account that only a quarter of the entire domain of definition was taken above and using the canonical equation of the second order surface (8), the result will not be trivial. $A_1x^2 + A_2y^2 + A_3z^2 + 2A_4yz + 2A_5zx +$

$$+2A_6xy + 2A_7x + 2A_8y + 2A_9z + A_{10} = 0 \quad (8)$$

$$(0; 0; 1020), (0; 90; 420), (0; -90; 420), (0; 45; 620), (90; 0; 400),$$
$$(-90; 0; 400), (90; 90; 170), (-90; 90; 170)$$
$$(90; -90; 170), (-90; -90; 170) \quad (9)$$

As you can see, in (8) there are transformations of the indicators in (9) and for convenience it is worth presenting them separately in (10).

$$(x^2; y^2; z^2; yz; zx; xy; x; y; z) =>$$
$$=> (0; 0; 1\,040\,400; 0; 0; 0; 0; 0; 1\,020),$$
$$(0; 8\,100; 176\,400; 37\,800; 0; 0; 0; 90; 420),$$
$$(0; 8\,100; 176\,400; -37\,800; 0; 0; 0; -90; 420),$$
$$(0; 2025; 384\,400; 27\,900; 0; 0; 0; 45; 620),$$
$$(8\,100; 0; 160\,000; 0; 36\,000; 0; 90; 0; 400),$$
$$(8\,100; 0; 160\,000; 0; -36\,000; 0; -90; 0; 400),$$
$$(8\,100; 8\,100; 28\,900; 15\,300; 15\,300; 8\,100; 90; 90; 170),$$
$$(8\,100; 8\,100; 28\,900; 15\,300; -15\,300; -8\,100; -90; 90; 170),$$

ISSN 2319-2836 (online), Published by
ASIA PACIFIC JOURNAL OF MARKETING & MANAGEMENT REVIEW.,
under Volume: 12 Issue: 11 in November-2023
https://www.gejournal.net/index.php/APJMMR

ASIA PACIFIC JOURNAL OF MARKETING & MANAGEMENT REVIEW
ISSN: 2319-2836
IMPACT FACTOR: 7.603
Vol 12, Issue 11, 2023

$$(8\,100; 8\,100; 28\,900; -15\,300; 15\,300; -8\,100; 90; -90; 170),$$
$$(8\,100; 8\,100; 28\,900; -15\,300; -15\,300; 8\,100; -90; -90; 170) \quad (10)$$

Thus, by means of these conclusions one can come to a solution (14).

$$(0; 0; 0; 0; 0; 0; 0; 0; 0; 0) \quad (14)$$

As a result of this part of the analysis, it was possible to come to the proof of the impossibility of representing the pattern of changes in the solar flux in a generally accurate form, resorting to general approximations according to (15).

$$E_s = E_{1.2} \pm \frac{E_1 - E_2}{181} * d = \begin{cases} E_1 + \frac{E_1 - E_2}{181} * d \\ E_2 - \frac{E_1 - E_2}{181} * d \end{cases} \quad (15)$$

$$Where, E_s - daily\ value\ of\ constant\ luminosity;$$
$$E_1 - luminosity\ in\ early\ January;$$
$$E_2 - luminosity\ in\ early\ July; d - number\ of\ days\ from\ the\ beginning\ of\ the\ year.$$

In this case, a value is indicated that defines it throughout the entire year, that is, taking the beginning of June or 181 days of the year as the peak, making some errors for a leap year. And for daily indicators it is defined as (16).

$$E_t = \left(\frac{|t_{12} - t|}{t_{12}} + \frac{|\alpha_0 - \alpha|}{\alpha_0}\right) * \frac{E_s}{2} \quad (16)$$

$$Where, t_{12} - exact\ time\ of\ noon; t - \ measurement\ time, action;$$
$$\alpha_0 - \ zero\ latitude\ (equator), equal\ to\ 90\ degrees;$$
$$\alpha - \ latitude\ at\ which\ measurements\ are\ taken$$
$$(south\ or\ north\ doesn't\ matter).$$

At the same time, it is worth paying tribute to the real model, which, even with all its approximateness, has a fairly high level of correlation with real empirical data. And if the analysis of the passage of radiation from the Sun to the receiver has been more or less analyzed, it is worth paying attention to the photometric characteristics. Of course, it is important to consider the issue from a variety of angles, including the wave and corpuscular theory, according to which the radiation flux is a set of quanta of real radiation, which ultimately form its flow, in this case the flux of light radiation (17), determined by through known constants, and the expression itself for determining the radiation flux, which is the ratio of the directed power over a certain period of time, is presented somewhat differently (18).

$$\Phi_v(\lambda) = K_m \sum_{i=1}^{N} V(\lambda_i) \cdot \Phi_e \quad (17)$$

$$\Phi_e(j) = \frac{dQ}{dt} = \frac{1}{dt} \int_{\nu_1}^{\nu_2} j(\lambda, \nu) \sum_{k=1}^{n_{j(\lambda)}} h\nu\, d\nu = \frac{1}{dt} \int_{\lambda_1}^{\lambda_2} j(\lambda) \sum_{k=1}^{n_{j(\lambda)}} \frac{hc}{\lambda} d\lambda = \Phi_e(\lambda) \quad (18)$$

In this case, the differential from the presented expression (19), and therefore integration over both, followed by substitution of the above-described expression, leads to the formation of (20).

ISSN 2319-2836 (online), Published by
ASIA PACIFIC JOURNAL OF MARKETING & MANAGEMENT REVIEW.,
under Volume: 12 Issue: 11 in November-2023
https://www.gejournal.net/index.php/APJMMR

ASIA PACIFIC JOURNAL OF MARKETING & MANAGEMENT REVIEW
ISSN: 2319-2836
IMPACT FACTOR: 7.603
Vol 12, Issue 11, 2023

$$d\Phi_v(\lambda) = K_m \sum_{i=1}^{N} V(\lambda_i) \cdot d\Phi_e(\lambda) \tag{19}$$

$$\Phi_v = K_m \int_{380\,nm}^{780\,nm} \sum_{i=1}^{N} V(\lambda_i) \cdot \Phi_e(\lambda)\, d\lambda =$$

$$= K_m \int_{380\,nm}^{780\,nm} \sum_{i=1}^{N} V(\lambda_i) \cdot \left[\frac{1}{dt} \int_{\lambda_1}^{\lambda_2} j(\lambda) \sum_{k=1}^{n_{j(\lambda)}} \frac{hc}{\lambda} d\lambda \right] d\lambda =$$

$$= \frac{K_m}{dt} \iint_{380\,nm}^{780\,nm} j(\lambda) \sum_{i=1}^{N} V(\lambda_i) \sum_{k=1}^{n_{j(\lambda)}} \frac{hc}{\lambda} (d\lambda)^2 \tag{20}$$

The obtained result may indicate that an increase in the concentration of directed radiation in a certain region through systems of lenses and also mirrors can lead to the fact that the number of quantum photons in this region will also increase. So, if we analyze real radiation as a two-dimensional projection, then at a distance within a certain radius, the area that the radiation will cover is proportional to the magnitude of the arc formed, in turn proportional to the scattering angle in radians (21).

$$\alpha = \frac{l}{r} = \left(\sum_{u_0=0}^{u} \int_{u_0}^{u} f(u,r) du dr \right) \cdot \left[\lim_{\Delta \vec{r} \to 0} r \right]^{-1} \tag{21}$$

However, moving to three-dimensional projection, it turns out that radiation (in each of the positions) comes from a certain point, falling from there onto an imaginary spherical surface, on which there is a certain two-dimensional Riemannian region or Riemannian plane on this spherical surface, to each point of which are drawn radii of the formed imaginary sphere. In this case, the area of this area with a known radius becomes known, and then the amount of energy or the number of photons released during such scattering from the specified point becomes proportional to the formed solid angle, which in turn is determined in (22).

$$\Omega = \frac{S}{r^2} = \left(\sum_{u_0'=0}^{u'} \oiint_{D'} S(u',r') dD' \right) \cdot \left[\lim_{\Delta \vec{r} \to 0} r \right]^{-2} \tag{22}$$

This conclusion is drawn from the fact that in a two-dimensional projection, during a decrease by 2 times, the length of the arc also decreases by 2 times, however, when measuring proportionality, for example, by the same 2 times, the area decreases by 4 times, that is, quadratically . From here we can preserve the same law of proportionality (24) for the output energy for each of the points, from which we can talk about introducing a certain energy function that describes the change in different areas of the resulting area of concentration of different energy photons (23).

$$E = h\nu = \frac{hc}{\lambda} \tag{23}$$

ISSN 2319-2836 (online), Published by
ASIA PACIFIC JOURNAL OF MARKETING & MANAGEMENT REVIEW.,
under Volume: 12 Issue: 11 in November-2023
https://www.gejournal.net/index.php/APJMMR

ASIA PACIFIC JOURNAL OF MARKETING & MANAGEMENT REVIEW
ISSN: 2319-2836
IMPACT FACTOR: 7.603
Vol 12, Issue 11, 2023

$$Q' \sim f(E,x) \iint_D \frac{S(x,y)}{r^2} dxdy = f(E,x) \iint_{x_0,y_0}^{x,y} \frac{S(x,y)}{r^2} dxdy \quad (24)$$

It can be seen that the present equation is general and suitable for radiation with a low level of monochromaticity, however, for a situation of high monochromaticity, the classical forms of the presented equations become suitable. In addition, it is worth pointing out that in this case, since the total radiation flux is divided into certain imaginary point sources, each of them can have its own individual luminous intensity (25).

$$I = \frac{d\Phi}{d\Omega} \quad (25)$$

In this case, it is the increase in luminous intensity in candelas that leads to the desired results with the determination of the exact energy of the incoming flux, from which the resulting concentrated radiation is directed, according to the diagram (Fig. 1) into one of the specific pots - photoelectric block, thermoelectric block or photo-magnetic -electrical unit through an electronic switching system.

High anomalous photovoltage block

After the formed and generated electrical voltage has been removed from the generating compartments, it is directed towards the voltage increasing system. In general, electrical power comes out of the system, described in (26) with a known current (27), which is then directed to the block to films of anomalous photovoltage or, more precisely, its generation.

$$Q = UIt = \left(\iiint_1^k \prod_{k=1}^{i} \frac{\partial U'(x,y,z,t)}{\partial t} dxdydz \lim_{i \to n} \sum_{i=1}^{n} \frac{\partial I(t)}{\partial t} \right)_{\frac{(q)}{dt}} \quad (26)$$

$$I = \iiint_1^k \prod_{k=1}^{i} \frac{\partial U'(x,y,z,t)}{\partial t} dxdydz \left(\lim_{i \to n} \sum_{i=1}^{n} \frac{\partial R(t)}{\partial t} \right)^{-1} = \frac{U}{R} \quad (27)$$

The law presented in (28) is, of course, valid and from where it is easy to deduce (29), which can lead to the statement that it is possible to increase the voltage of the circuit (30) when electric current passes through ultrathin conductive films, which organize high resistance due to their small, almost molecular, increasing thickness and the creation under the influence of charges and the corresponding tension (31) of a potential difference (32), which, as can be seen from the formulation, can be described.

$$R = \iiint_1^{\alpha} \prod_{\alpha=1}^{\beta} \frac{\partial \rho'(x,y,z)}{\partial c} dxdydz \left(\lim_{\beta \to \gamma} \sum_{\gamma=1}^{n} \frac{\partial k(l)}{\partial l} \times \left(\frac{(\Delta s)}{\sin \varepsilon \, dt} \right)^{-1} \right) = \rho \frac{l}{s} \quad (28)$$

$$E = \frac{w'}{\partial w} \iiint_1^k \prod_{k=1}^{i} \frac{\partial F'(x,y,z,t)}{\partial t} dxdydz \left(\lim_{i \to n} \sum_{i=1}^{n} \frac{\partial q(t)}{\partial t} \right)^{-1} = \frac{F}{q} \quad (29)$$

$$U = \varphi_2 - \varphi_1 =$$

ISSN 2319-2836 (online), Published by
ASIA PACIFIC JOURNAL OF MARKETING & MANAGEMENT REVIEW.,
under Volume: 12 Issue: 11 in November-2023
https://www.gejournal.net/index.php/APJMMR

ASIA PACIFIC JOURNAL OF MARKETING & MANAGEMENT REVIEW
ISSN: 2319-2836
IMPACT FACTOR: 7.603
Vol 12, Issue 11, 2023

$$= \iiint_{1}^{k} \prod_{k=1}^{i} \frac{\partial k'(x,y,z,t)}{\partial t} dxdydz \left(\lim_{i \to n} \sum_{i=1}^{n} \frac{\partial r(x)}{\partial x} \right)^{-2} ** \left(\left(\lim_{i \to n} \sum_{i=1}^{n} \frac{\partial q_1(t)}{\partial t} \right) - \left(\lim_{i \to n} \sum_{i=1}^{n} \frac{\partial q_2(t)}{\partial t} \right) \right)$$

$$=$$

$$= \frac{kq_1}{r^2} - \frac{kq_2}{r^2} \tag{30}$$

However, in this case it becomes necessary to determine the charge values (31), because since the voltage or potential difference (32) increases, the current strength (33), according to the same equation, must decrease, which is also visible when expressed through the same value charge in an equation with disclosure.

$$q = \int_{1}^{\beta'} \left(\lim_{\beta \to \gamma} \sum_{\gamma=1}^{n} \frac{\partial A_{\beta,\gamma}(x,y,z,t)}{\partial l} \times \left(\frac{U(\Delta\varphi,x,y,z,t)}{\sin \varepsilon \, dt} \right)^{-1} \right) d\nabla = \frac{A}{U} \tag{31}$$

$$I = \frac{w'}{\partial w} \iiint_{1}^{k} \prod_{k=1}^{i} \frac{\partial q'(\nabla,t)}{\partial t} dxdydz \left(\lim_{i \to n} \sum_{i=1}^{n} \frac{\partial(t)}{\partial t} \right)^{-1} = \frac{q}{t} \tag{32}$$

Finally, after passing through such a system, with a sufficiently high efficiency, it becomes realistic to determine the output power (33) for a converted electric current with an abnormally high voltage and low current, which was required when designing the solar optron device system.

$$P = \int_{1}^{\beta'} \left(\lim_{\beta \to \gamma} \sum_{\gamma=1}^{n} \frac{\partial I_{\beta,\gamma}(x,y,z,t)}{\partial l} \times \left(\frac{U(\Delta\varphi,x,y,z,t)}{\sin \varepsilon \, dt} \right) \right) d\nabla = UI \tag{33}$$

Conclusion

As a result of the analysis, it was possible to follow the entire design and algorithm, which analyzed this entire system from the physical and mathematical side.

A complete description of the helioptotron device, which receives solar radiation, was obtained to predict changes in the original flux shape throughout the year.

Subsequently, by a system for increasing the flux of light radiation, further transformation, by directing it through fiber optic and photoelectric connections to converters of this radiation into electric current.

An analysis of each of the processes is provided, from the photoelectric effect, operating in the first model with its own individual mathematical apparatus, also in the thermoelectric system, with a description of the method of using thermoelements with its own calculation algorithms.

Photoelectric and conductive connections are briefly described, with a further transition to the representation of a mathematical model for films with the generation of anomalous photovoltage, which was subsequently achieved by describing the presented quantum-molecular physical and mathematical systems of matrix-functional differential-integral equations. Thus, we can talk about conducting a complete analysis of the solar optron device system with all its features and aspects.

REFERENCES:

ISSN 2319-2836 (online), Published by
ASIA PACIFIC JOURNAL OF MARKETING & MANAGEMENT REVIEW.,
under Volume: 12 Issue: 11 in November-2023
https://www.gejournal.net/index.php/APJMMR

1. Артемьев, Юрий Фотохимия твердого тела / Юрий Артемьев. - М.: Санкт-Петербургский государственный университет, 2018. - 874 с.
2. Ахманов, С. А. Физическая оптика / С.А. Ахманов, С.Ю. Никитин. - М.: Издательство МГУ, Наука, 2018. - 654 с.
3. Бабенко, С. П. Дифракция световых волн. Учебное пособие / С.П. Бабенко. - М.: МГТУ им. Н. Э. Баумана, 2018. - 48 с.
4. Кораблев В. А., Тахистов Ф. Ю., Шарков А. В. Прикладная физика. Термоэлектрические модули и устройства на их основе: Учебное пособие / Под ред. проф. А. В. Шаркова. СПб: СПбГИТМО (ТУ), 2003.
5. Тахистов Ф. Ю., Гершберг И. А. Оптимизация параметров термоэлектрического генераторного модуля с учетом эффективности теплообмена на сторонах модуля // Термоэлектрики и их применения. Доклады XI Межгосударственного семинара. СПб: ФТИ, 2008.
6. Ерофеев Р. С. Влияние термоэлектрических явлений на тектонические процессы и климат Земли // Термоэлектричество. 2010. № 1.
7. Шостаковский П. Современные решения термоэлектрического охлаждения для радиоэлектронной, медицинской, промышленной и бытовой техники // Компоненты и технологии. 2009. № 12. 2010. № 1.
8. Нефедов, А.И. Внутреннее электромагнитное поле человека и биоэлектромагнетизм / А.И. Нефедов. - М.: Русайнс, 2014. - 352 с.
9. O.S. Rayimjonova, Kh.T. Yuldashev, U.Sh. Ergashev, G.F. Jurayeva, L.R. Dalibekov Photo Converter for Research of Characteristics Laser IR Radiation // International Journal of Advanced Research in Science, Engineering and Technology Vol. 7, Issue 2 , February 2020. pp. 12788-12791
10. Nurdinova Raziyakhon Abdikhalikovna, Rayimjonova Odinahon Sodikovna. Ergashev Shohbozjon Umarali ugli, Tillaboyev Muhiddin G'anijonovich. ANOMALOUS PHOTOVOLTAIC EFFECT IN DIELECTRICS, International Journal of Advance Scientific Research. VOLUME 02 ISSUE 06 Pages: 96-102 2022.
11. Тургунов Б. А., Эргашев Ш., Орифжонова Д. В. Основные проблемы //Коммуникативные стратегии информационного общества. – 2019. – С. 179-181.
12. Rayimjonova O. S., Tillaboyev M. G., Xusanova S. S. UNDERGROUND WATER DESALINATION DEVICE //International Journal of Advance Scientific Research. – 2022. – Т. 2. – №. 12. – С. 59-63.

ISSN 2319-2836 (online), Published by
ASIA PACIFIC JOURNAL OF MARKETING & MANAGEMENT REVIEW.,
under Volume: 12 Issue: 11 in November-2023
https://www.gejournal.net/index.php/APJMMR